Catal Lett (2012) 142:118–123
DOI 10.1007/s10562-011-0735-7

Dynamic Behavior of Pd Species in an $LaFe_{0.95}Pd_{0.05}O_3$ Perovskite

Xiaojing Zhang · Huaju Li · Yong Li · Wenjie Shen

Received: 30 July 2011 / Accepted: 2 November 2011 / Published online: 11 November 2011

Abstract $LaFe_{0.95}Pd_{0.05}O_3$ prepared by a sol–gel process was stable under reducing atmospheres up to 1,073 K. Under reducing atmospheres metallic palladium left the $LaFeO_3$ lattice and ionic palladium was reversibly incorporated into the perovskite framework in oxidizing environments. The catalytic activity of $LaFe_{0.95}Pd_{0.05}O_3$ was higher than that of $LaFeO_3$.

Keywords Heterogeneous catalysis · Perovskite · $LaFeO_3$ · Pd doping · CO oxidation

1 Introduction

Pd-containing perovskites have attracted increasing attention as potential automotive catalysts for vehicle exhaust abatement. Doping very small amounts of Pd into $LaFeCoO_3$ and $LaFeO_3$ perovskites significantly improved the catalytic durability; these doped materials are referred to as intelligent perovskites [1, 2]. For example, $LaFe_{0.57}Co_{0.38}Pd_{0.05}O_3$, even after long-term ageing at 1,173 K, still displayed superior activity and stability to those of a Pd/Al_2O_3 catalyst [1]. The palladium content of this intelligent catalyst was 70% less than those of commercial catalysts. It was proposed that Pd species, in response to inherent redox fluctuations in automobile exhausts, were reversibly and rapidly incorporated into and removed from the perovskite lattice [1–4]. This self-regenerative function suppressed the sintering of Pd grains, which is the major cause of deactivation of current automotive catalysts. Pd-doped $LaMnO_3$ [5] and $LaCoO_3$ [6] perovskites have also been confirmed to efficiently suppress the sintering of Pd species, but their structures were less stable under reducing atmospheres at high temperatures, especially in the case of Pd–$LaCoO_3$ [7, 8]. However, the dynamic behavior of Pd species in response to changes in oxidizing and reducing atmospheres is still not well understood with respect to chemical states and diffusion mechanisms.

CO is one of the major pollutants in automobile exhausts. In most cases, the addition of Pd to a perovskite, either on the surface or within the perovskite lattice, enhances the catalytic activity towards CO oxidation, as demonstrated by Pd doping of $BaCeO_3$ [9], $YFeO_3$ [10], and $LaFeO_3$ [11]. However, it was also occasionally observed that Pd incorporation into $LaCoO_3$ resulted in inferior activity for CO oxidation [6]. In this work, we investigated the dynamic behavior of Pd pieces in an $LaFe_{0.95}Pd_{0.05}O_3$ perovskite under reducing and oxidizing atmospheres. High-resolution transmission electron microscopy (HRTEM) observations provided direct evidence of reversible movement of the Pd species out of and into the perovskite structure, and X-ray photoelectron spectroscopy (XPS) quantitatively verified the changes in the coordination environment of the Pd species. The physicochemical properties induced by Pd doping into $LaFeO_3$ correlated with catalytic performance in CO oxidation.

2 Experimental

2.1 Catalyst Preparation

The $LaFe_{1-x}Pd_xO_3$ perovskites ($x = 0$ and 0.05) were prepared by a sol–gel process. Typically, 75 mL of an

X. Zhang · H. Li · Y. Li · W. Shen (✉)
State Key Laboratory of Catalysis, Dalian Institute of Chemical Physics, Chinese Academy of Sciences, Dalian 116023, China
e-mail: shen98@dicp.ac.cn

aqueous solution containing La^{3+}, Fe^{3+}, and Pd^{2+} in molar ratios of $1/(1-x)/x$ were slowly added to 40 mL of an aqueous solution of EDTA/citric acid/ammonia. The metal ions/EDTA/citric acid molar ratios were fixed at 1/1/1.5. Then 12 mL of 14.7 M aqueous ammonia solution were added to the mixture to give a final pH value of 4.0. The mixture was refluxed at 353 K for 6 h under stirring, and the excess water slowly evaporated. The resulting sol was dried at 373 K overnight, and calcined at 723 K for 3 h and at 1,073 K for 5 h in air. For comparison, a reference sample of $Pd/LaFeO_3$ with the same Pd loading as the $LaFe_{0.95}Pd_{0.05}O_3$ sample (2.2 wt% Pd) was prepared by impregnating $LaFeO_3$ with an aqueous solution of $Pd(NO_3)_2$ and calcining at 873 K for 3 h in air.

2.2 Catalyst Characterization

Nitrogen adsorption–desorption isotherms were recorded at 77 K on a Nova 4200e instrument. Before the measurements, the samples were degassed at 573 K for 6 h. The specific surface areas were calculated by multipoint BET analysis of the nitrogen adsorption isotherms.

X-ray powder diffraction (XRD) patterns were recorded on a Rigaku D/MAX-RB diffractometer with a Cu Kα radiation source operated at 40 kV and 250 mA. In situ XRD measurements were conducted in a high-temperature chamber. The sample was pressed into a self-supporting flake and mounted in the chamber. A 20% H_2/N_2 mixture was introduced into the chamber and the sample was heated at a ramp rate of 5 K/min, during which XRD patterns were recorded at the desired temperatures. The mean crystallite size was calculated from the Scherrer equation [12].

Temperature-programmed desorption of oxygen (O_2-TPD) was tested with a microreactor connected to a mass spectrometer (OmniStar 200). A sample (100 mg; 40–60 mesh) was pre-treated with a 20% O_2/He mixture (flow rate 20 mL/min) at 973 K for 1 h. After cooling to room temperature, the sample was heated to 1,173 K at a ramp rate of 10 K/min under a He flow (flow rate 20 mL/min). Oxygen desorption was monitored by the mass spectrometer.

Temperature-programmed reduction of hydrogen (H_2-TPR) was performed using a microreactor equipped with a thermal conductivity detector (TCD). A sample (100 mg; 40–60 mesh) was pre-treated with a 20% O_2/He mixture (flow rate 20 mL/min) at 973 K (873 K for the $Pd/LaFeO_3$ sample) for 1 h to remove the adsorbed carbonates and hydrates. After cooling to room temperature, the sample was exposed to a 5% H_2/N_2 mixture (flow rate 30 mL/min) and then heated up to 1,073 K at a ramp rate of 10 K/min. The oxygen storage capacity (OSC) was measured with the same equipment by reducing the sample at 1,073 K with a 5% H_2/N_2 mixture (flow rate 30 mL/min), followed by pulsing O_2 periodically at 773 K until saturation.

XP spectra were recorded on a VG ESCALAB MK II instrument using an Al Kα excitation source. When necessary, the sample was reduced in the chamber with a 10% H_2/N_2 mixture at 773 K for 1 h. The charging effect was corrected by referencing the binding energy of La $3d_{5/2}$ at 833.7 eV [8].

HRTEM images were obtained using an FEI Tecnai G2 F30 S-Twin microscope operated at an acceleration voltage of 300 kV. The specimen was prepared by ultrasonically dispersing the powder sample into *n*-hexane and droplets of the suspensions were deposited onto the copper grid and dried in air.

2.3 CO Oxidation

CO oxidation was tested with a fixed-bed quartz tubular reactor at atmospheric pressure. The catalyst (100 mg; 40–60 mesh) was loaded into the reactor and the feed gas (1% CO/20% O_2/He, flow rate 30 mL/min) was introduced through a mass flow controller with a gas hourly space velocity (GHSV) of 18 000 mL/(g_{cat} h). Effluent from the reactor was analyzed using an online gas chromatograph equipped with a TCD and a flame ionization detector (FID). To determine the concentration of CO_2 produced quantitatively, a nickel catalytic converter was placed before the FID and used to convert CO_2 into methane.

3 Results and Discussion

3.1 Structural Properties

Figure 1 shows the XRD patterns of the $LaFeO_3$ and $LaFe_{0.95}Pd_{0.05}O_3$ samples. Typical diffraction lines of orthorhombic $LaFeO_3$ (JCPDS 88-0641) were clearly observed in both cases. The crystallite sizes of the two samples were about 40 nm, as estimated from the most intense (121) reflections. The magnified diffraction at 2θ of 31.9–32.6° shifted to a slightly higher angle in the $LaFe_{0.95}Pd_{0.05}O_3$ sample, indicating distortion of the crystal cell as a result of the insertion of Pd ions. This is similar to the cases of Pd–$LaCoO_3$ [7] and $LaFe_{0.77}Co_{0.17}Pd_{0.06}O_3$ [13]. The specific surface areas were 6.4 and 5.2 m^2/g^{-1} for $LaFeO_3$ and $LaFe_{0.95}Pd_{0.05}O_3$, respectively, suggesting that Pd substitution at the B-sites of $LaFeO_3$ only marginally reduced the surface area.

Figure 2 illustrates the O_2–TPD profiles of the $LaFeO_3$ and $LaFe_{0.95}Pd_{0.05}O_3$ catalysts. Usually, there are two types of oxygen desorptions, corresponding to α- and β-oxygen species in perovskites [14, 15]. The α-oxygen is related to the surface oxygen species that desorb at lower temperatures; α-oxygen exists in perovskites with partial substitution of the A-site ions. The β-oxygen is associated with

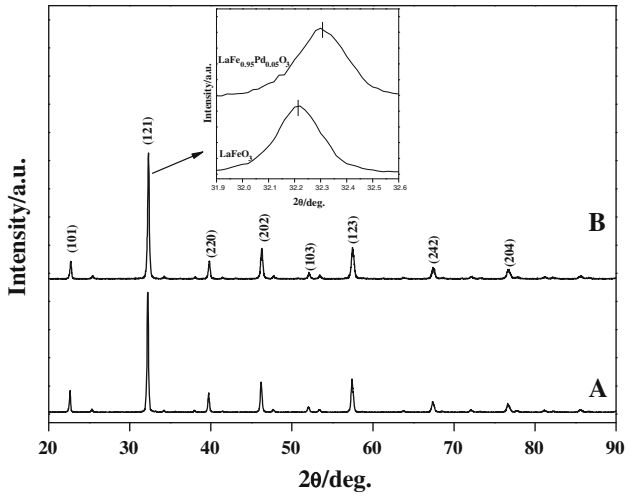

Fig. 1 XRD patterns of *a* $LaFeO_3$,and *b* $LaFe_{0.95}Pd_{0.05}O_3$

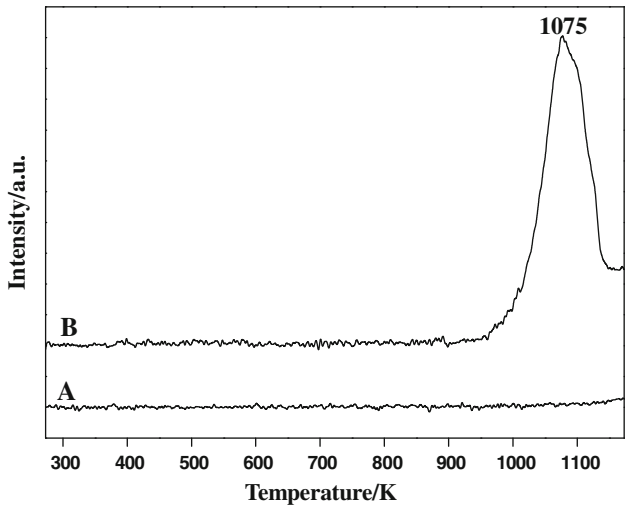

Fig. 2 O_2-TPD profiles of *a* $LaFeO_3$, and *b* $LaFe_{0.95}Pd_{0.05}O_3$

reduction of the B-site ions and desorbs at relatively high temperatures. For $LaFeO_3$, only traces of β-oxygen were detected, in agreement with the general understanding that $LaFeO_3$ hardly releases oxygen species below 1,073 K [15]. However, significant desorption of β-oxygen appeared at 1,075 K on the $LaFe_{0.95}Pd_{0.05}O_3$ sample, suggesting that Pd substitution had promoted the mobility of the lattice oxygen, which diffused from the bulk to the surface. This was further supported by the OSCs of the samples. The OSC of $LaFeO_3$ was 320 μmol-O_2/g, and it increased significantly to 444 μmol-O_2/g for $LaFe_{0.95}Pd_{0.05}O_3$.

Figure 3 compares the H_2-TPR profiles of the $LaFeO_3$ and $LaFe_{0.95}Pd_{0.05}O_3$ catalysts. Two reduction peaks of $LaFeO_3$ appeared at 761 and 901 K as a result of reduction of Fe^{3+} to Fe^{2+} on the surface and in the bulk [14], respectively. The reduction behavior of $LaFe_{0.95}Pd_{0.05}O_3$

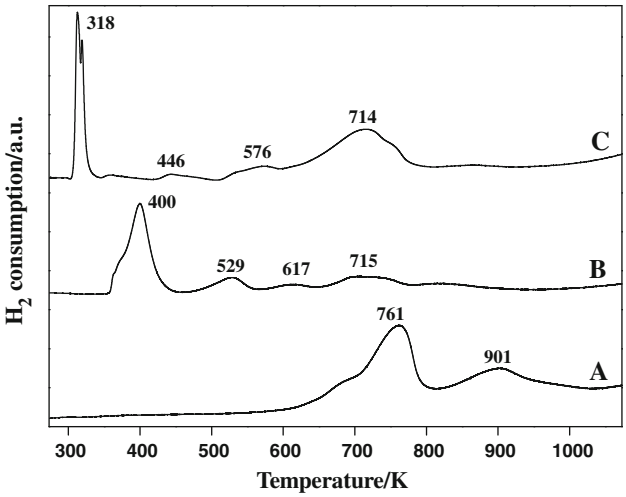

Fig. 3 H_2-TPR profiles of *a* $LaFeO_3$, *b* $LaFe_{0.95}Pd_{0.05}O_3$, and *c* Pd/$LaFeO_3$

was somewhat complicated. The peak at 400 K was attributed to reduction of Pd^{n+} species within the perovskite to metallic Pd [16]. The weak peak at 529 K represented the reduction of a small amount of Fe^{4+}, which was generated to compensate for charge imbalance on Pd doping [14, 17]. The two minor peaks at 617 and 715 K corresponded to the reduction of Fe^{3+} to Fe^{2+} on the surface and in the bulk of the perovskite. For the reference Pd/$LaFeO_3$ catalyst, PdO was readily reduced to metallic Pd at 318 K. The minor peak at 446 K was assigned to the reduction of Pd^{n+} incorporated into the perovskite structure [18]. The peak at 714 K corresponded to reduction of Fe^{3+} to Fe^{2+} in the perovskite. The temperature at which reduction of PdO species in the $LaFe_{0.95}Pd_{0.05}O_3$ perovskite occurred was higher (400 K) than that for PdO in the reference Pd/$LaFeO_3$ catalyst (318 K).

3.2 Dynamic Behavior of Pd Species

Figure 4 shows the XPS spectra of Pd 3d in the $LaFe_{0.95}Pd_{0.05}O_3$ and Pd/$LaFeO_3$ samples. The binding energy of Pd $3d_{5/2}$ in the as-prepared $LaFe_{0.95}Pd_{0.05}O_3$ was 337.1 eV; this is higher than that of Pd^{2+} (336.8 eV) but lower than that of Pd^{4+} (337.7 eV) [19]. Based on the narrow width (FWHM = 1.92 eV) and the symmetry of the Pd $3d_{5/2}$ peak, the Pd species were defined as Pd^{n+} ($2 < n < 4$), located at the B-sites [9, 16]. In contrast, the binding energy of Pd $3d_{5/2}$ (336.8 eV) in the reference Pd/$LaFeO_3$ sample was characteristic of PdO. After reduction with hydrogen at 773 K, the binding energies of Pd $3d_{5/2}$ in both samples shifted to 335.4 eV, indicative of metallic Pd [19]. This result confirmed that the Pd^{n+} species in $LaFe_{0.95}Pd_{0.05}O_3$ had been readily reduced to metallic Pd, which was then segregated from the B-sites and

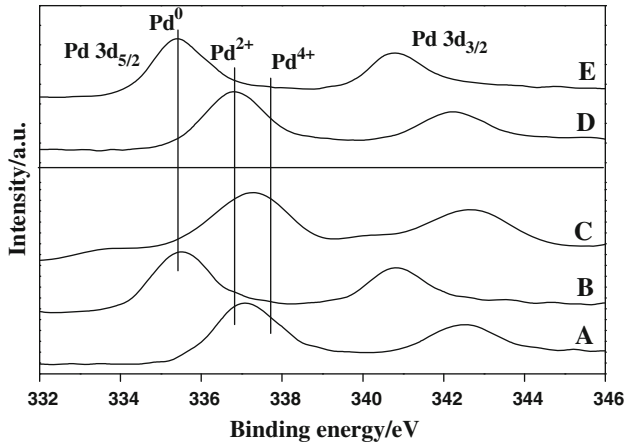

Fig. 4 XPS spectra of Pd 3d in the $LaFe_{0.95}Pd_{0.05}O_3$ catalysts, *a* as-prepared, *b* hydrogen-reduced at 773 K, and *c* consecutive reduction–oxidation, and in the Pd/$LaFeO_3$ catalysts: *d* as-prepared, and *e* hydrogen-reduced at 773 K

dispersed on the surface. On re-oxidation at 1,073 K, the binding energy of Pd $3d_{5/2}$ in $LaFe_{0.95}Pd_{0.05}O_3$ shifted to 337.3 eV, suggesting that metallic Pd had been oxidized to PdO species.

This phenomenon was further supported by HRTEM observations. As shown in Fig. 5, the as-prepared $LaFe_{0.95}Pd_{0.05}O_3$ sample contained agglomerated particles with an average size of about 80 nm. The fringe spaces of 0.393 and 0.783 nm corresponded to the {101} and {010} planes of $LaFeO_3$, respectively. The selected area electron diffraction (SAED) pattern confirmed that the sample was a single crystal with an orthorhombic structure. After reduction with hydrogen at 773 K, Pd particles 3–8 nm in diameter appeared on the perovskite surface. The fringe spacing of 0.227 nm suggested that the Pd particles exposed the {011} plane. On further increasing the reduction temperature to 1,073 K, the size of the Pd particles increased to 11–15 nm. This result clearly indicated that the Pd species segregated from the perovskite framework on reduction with hydrogen and existed as metallic particles on the surface. The sample after re-oxidation at 1,073 K showed a similar morphology to that of the as-prepared sample, but the Pd particles had entirely disappeared, confirming that re-oxidation caused the Pd particles to diffuse into the perovskite lattice. Based on these results, it can be proposed that Pd species in $LaFe_{0.95}Pd_{0.05}O_3$ can move reversibly out of/into the perovskite structure in response to reducing/oxidizing atmospheres. The chemical state of the Pd species varied between metallic palladium after reduction, and palladium oxide within the perovskite structure on re-oxidation.

Figure 6 shows the in situ XRD patterns of the $LaFe_{0.95}Pd_{0.05}O_3$ sample during reduction with hydrogen. The perovskite structure of $LaFe_{0.95}Pd_{0.05}O_3$ was stable up

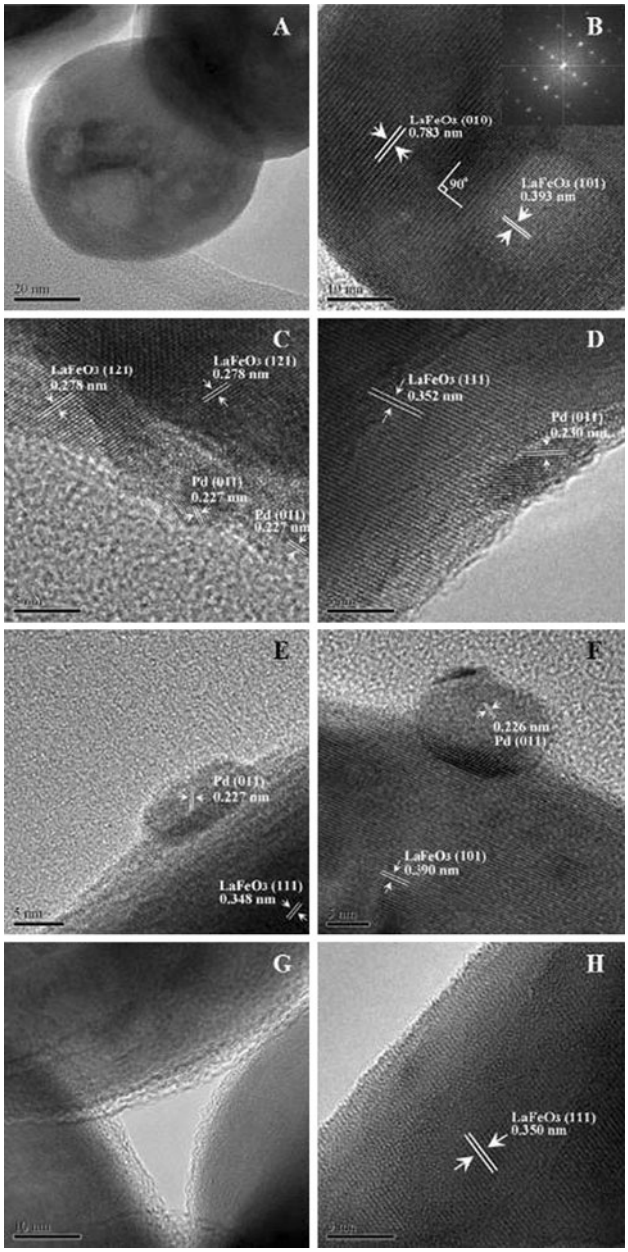

Fig. 5 HRTEM micrographs of the $LaFe_{0.95}Pd_{0.05}O_3$ catalysts **a, b** as-prepared, **c, d** hydrogen- reduced at 773 K, **e, f** hydrogen reduced at 1,073 K, and **g, h** consecutive reduction–oxidation

to 1,073 K and the crystallite sizes were about 40 nm. The magnified XRD patterns of the most intense (121) reflections showed that the 2θ positions in the range 32.08–32.10° remained unchanged from 473 to 1,073 K, suggesting that Pd segregation from the perovskite framework did not obviously alter the perovskite structure.

3.3 CO Oxidation

Figure 7 compares the catalytic performances of the $LaFeO_3$ and $LaFe_{0.95}Pd_{0.05}O_3$ samples for CO oxidation.

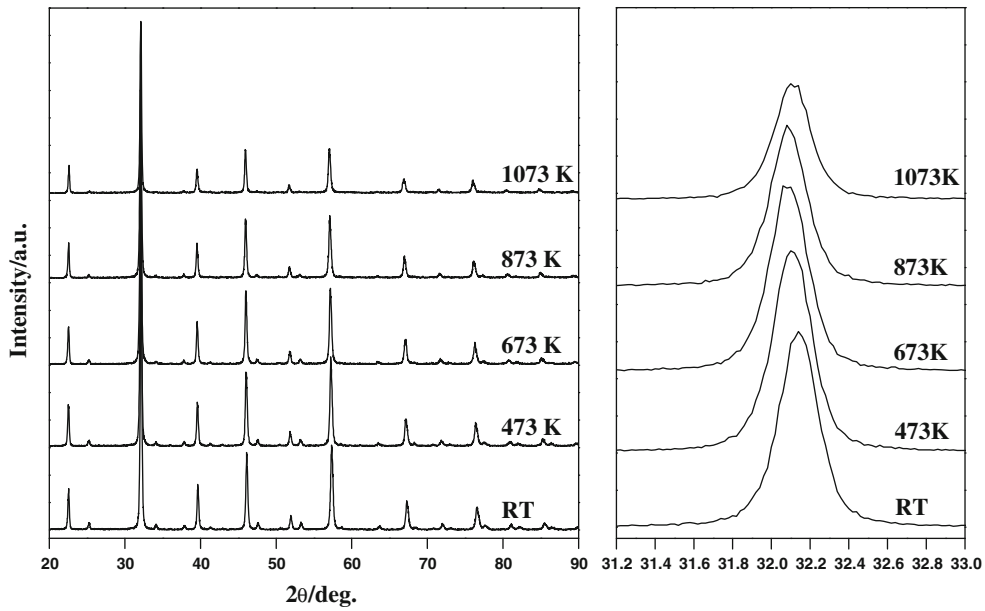

Fig. 6 *In-situ* XRD patterns of $LaFe_{0.95}Pd_{0.05}O_3$ reduced with a 20% H_2/N_2 mixture

$LaFeO_3$ was almost inert in the temperature range investigated. $LaFe_{0.95}Pd_{0.05}O_3$ gave 50% CO conversion at 475 K (T_{50}) and 100% conversion at 483 K (T_{100}), demonstrating that the main contribution to CO oxidation was derived from the Pd species. Enhanced activities towards CO oxidation were also observed on $BaCe_{0.90}Pd_{0.10}O_3$ [9], $YFe_{0.90}Pd_{0.10}O_3$ [10], and $LaFePd_{0.05}O_3$ [11]. The Pd species located at the perovskite lattice [9, 10] or dispersed on the perovskite surface [11] were considered to be the active sites for CO oxidation. The Pd species located at the perovskite lattice were responsible for the activity improvement in CO oxidation.

When the $LaFe_{0.95}Pd_{0.05}O_3$ catalyst was reduced with hydrogen at 573 K, the activity was further enhanced, with a T_{50} of 435 K and a T_{100} of 443 K. However, the $LaFe_{0.95}Pd_{0.05}O_3$ sample that was subjected to reduction with hydrogen at 573 K followed by re-oxidation at 773 K displayed almost the same activity as that of the as-prepared $LaFe_{0.95}Pd_{0.05}O_3$. This reaction pattern suggested that the activity of $LaFe_{0.95}Pd_{0.05}O_3$ in CO oxidation was closely associated with the chemical state of the Pd species. On reduction with hydrogen, Pd particles segregated from the perovskite lattice, as confirmed by the H_2-TPR, XPS, and HRTEM measurements, and were more active for CO oxidation than were the PdO species within the perovskite lattice, lowering the T_{50} by 40 K. A similar phenomenon has been observed for $LaCo_{0.95}Pd_{0.05}O_3$: reduction with hydrogen at 453 K lowered the T_{50} by 43 K in CO oxidation [6]. In contrast, the activity for CO oxidation decreased on a $BaCe_{0.90}Pd_{0.10}O_3$ perovskite [9] and was almost unaffected on a $YFe_{0.90}Pd_{0.10}O_3$ perovskite [10] on reduction with hydrogen at high temperatures. For

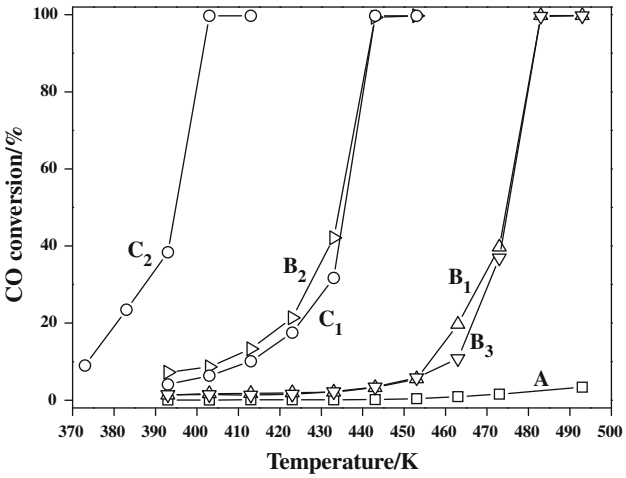

Fig. 7 CO oxidation on *a* $LaFeO_3$, and *b* $LaFe_{0.95}Pd_{0.05}O_3$: B_1 as-prepared, B_2 pre-reduced, B_3 consecutive reduction–oxidation; and *c* $Pd/LaFeO_3$: (C_1) as-prepared and (C_2) pre-reduced. Reaction conditions: 1% CO/20% O_2/He, 18,000 mL/(g_{cat} h)

comparison, CO oxidation was tested on the reference $Pd/LaFeO_3$ catalyst. The as-prepared $Pd/LaFeO_3$ sample showed a T_{50} of 435 K and a T_{100} of 443 K; these values were much lower than those obtained on the as-prepared $LaFe_{0.95}Pd_{0.05}O_3$ catalyst. This indicated that PdO species dispersed on the perovskite surface were more active for CO oxidation than those incorporated into the perovskite lattice. On reduction with hydrogen at 573 K, the $Pd/LaFeO_3$ catalyst gave a T_{50} of 395 K and a T_{100} of 403 K, further confirming that Pd particles on the perovskite surface were more active for CO oxidation than those in the lattice were.

Notably, the activity of the reduced $Pd/LaFeO_3$ catalyst was superior to that of the reduced $LaFe_{0.95}Pd_{0.05}O_3$ catalyst. This was a result of the different bonding patterns of the Pd particles on the substrate after reduction with hydrogen at 573 K. On the reduced $Pd/LaFeO_3$ catalyst, Pd particles were derived from the previously dispersed PdO particles, almost without involving reduction of the $LaFeO_3$ support. In the case of the reduced $LaFe_{0.95}Pd_{0.05}O_3$ catalyst, however, Pd particles were segregated from the perovskite lattice, and at the same time the $LaFeO_3$ support was also partially reduced, as confirmed by the H_2-TPR measurements. CO oxidation on perovskite-type oxides follows a suprafacial mechanism; this requires participation of the surface oxygen. On the reduced $Pd/LaFeO_3$ sample, CO adsorbed on the Pd particles and reacted directly with the surface oxygen on the support, forming CO_2. On the reduced $LaFe_{0.95}Pd_{0.05}O_3$ catalyst, however, the surface oxygen strongly interacted with the perovskite and therefore a smaller amount of surface oxygen was available for CO oxidation, resulting in lower activity.

4 Conclusion

Pd doping into $LaFeO_3$ significantly promoted the thermal stability of the perovskite and the mobility of oxygen species. The Pd species in the $LaFe_{0.95}Pd_{0.05}O_3$ perovskite reversibly moved out of/into the framework in response to changes in the reducing/oxidizing atmospheres. The $LaFe_{0.95}Pd_{0.05}O_3$ catalyst, either as-prepared or pre-reduced with hydrogen, showed considerably enhanced activities for CO oxidation compared with that of the parent $LaFeO_3$ perovskite.

References

1. Nishihata Y, Mizuki J, Akao T, Tanaka H, Uenishi M, Kimura M, Okamoto T, Hamada N (2002) Nature 418:164
2. Tanaka H, Taniguchi M, Kajita N, Uenishi M, Tan I, Sato N, Narita K, Kimura M (2004) Top Catal 30/31:389
3. Uenishi M, Tanaka H, Taniguchi M, Tan I, Nishihata Y, Mizuki J, Kobayashi T (2008) Catal Commun 9:311
4. Matsumura D, Nishihata Y, Mizuki J, Taniguchi M, Uenishi M, Tanaka H (2010) J Appl Phys 107:124319
5. Cimino S, Casaletto MP, Lisi L, Russo G (2007) Appl Catal A 327:238
6. Sartipi S, Khodadadi AA, Mortazavi Y (2008) Appl Catal B 83:214
7. Chiarello GL, Grunwaldt JD, Ferri D, Krumeich F, Oliva C, Forni L, Baiker A (2007) J Catal 252:127
8. Twagirashema I, Engelmann-Pirez M, Frere M, Burylo L, Gengembre L, Dujardin C, Granger P (2007) Catal Today 119:100
9. Singh UG, Li J, Bennett JW, Rappe AM, Seshadri R, Scott SL (2007) J Catal 249:349
10. Li J, Singh UG, Schladt TD, Stalick JK, Scott SL, Seshadri R (2008) Chem Mater 20:6567
11. Ziaei-Azad H, Khodadadi A, Esmaeilnejad-Ahranjani P, Mortazavi Y (2011) Appl Catal B 102:62
12. Cullity BD (1978) Elements of X-Ray Diffraction, 2nd edn. Addison-Wesley, Menlo Park
13. Zhou KB, Chen HD, Tian Q, Hao ZP, Shen DX, Xu XB (2002) J Mol Catal A 189:225
14. Zhang RD, Villanueva A, Alamdari H, Kaliaguine S (2006) J Catal 237:368
15. Rossetti I, Forni L (2001) Appl Catal B 33:345
16. Uenishia M, Taniguchi M, Tanaka H, Kimura M, Nishihata Y, Mizuki J, Kobayashi T (2005) Appl Catal B 57:267
17. Ciambelli P, Cimino S, De Rossi S, Lisi L, Minelli G, Porta P, Russo G (2001) Appl Catal B 29:239
18. Eyssler A, Mandaliev P, Winkler A, Hug P, Safonova O, Figi R, Weidenkaff A, Ferri D (2010) J Phys Chem C 114:4584
19. Giraudon JM, Elhachimi A, Wyrwalski F, Siffert S, Aboukais A, Lamonier JF, Leclercq G (2007) Appl Catal B 75:157